STRONGLY INTERACTING ELECTROWEAK SECTOR AT A MUON COLLIDER

V. BARGER AND T.HAN

Physics Department, University of Wisconsin, Madison, WI 53706, USA

We discuss the excellent prospects for a detailed study of a strongly interacting electroweak sector at a muon collider with c.m. energy $\sqrt{s} \sim 4$ TeV. For expected luminosity of $L = 200 - 1000$ fb^{-1} per year, $\mu^+\mu^-$ and $\mu^+\mu^+$ (or $\mu^-\mu^-$) collisions can be used to study longitudinal W^+W^- and W^+W^+ (or W^-W^-) scattering with considerable precision.

1 Introduction

Despite the extraordinary success of the Standard Model (SM) in describing particle physics up to the highest energy available today, the nature of electroweak symmetry-breaking (EWSB) remains undetermined. In particular, it is conceivable that there is no light ($\lesssim$ 700 GeV) Higgs boson. General arguments [1] based on partial wave unitarity then imply that the $W^\pm, Z$ electroweak gauge bosons develop strong (non-perturbative) interactions by energy scales of order 1–2 TeV. For a collider to probe such energy scales, the c.m. energy must be sufficient that gauge-boson scattering (see Fig. 1) at subprocess energies at or above 1 TeV occurs with substantial frequency. The only colliders under construction or being planned that potentially meet this requirement are the CERN LHC, a future linear e^+e^- collider with $\sqrt{s} \lesssim 1.5$ TeV (NLC), and a high energy muon collider (NMC).

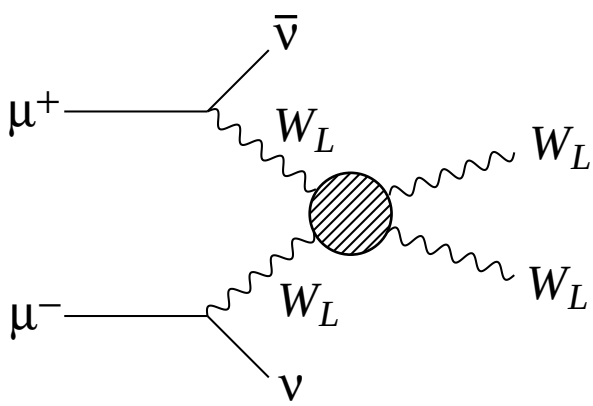

Figure 1. Symbolic diagram for strong VV scattering.

The ability to extract signals and learn about a strongly-interacting-electroweak sector (SEWS) at the LHC and NLC has been the subject of many studies [2,3,4,5,6]. The conclusion is that the LHC and NLC will yield first evidence for a SEWS theory, but for many models

the evidence will be of rather marginal statistical significance. SEWS models yielding large signals (such as the Standard Model with a 1 TeV Higgs boson or a model with a spin-1, isospin-1 resonance at 1 TeV) will be readily apparent or easily eliminated, but models that yield only a small number of excess events will be very difficult to distinguish from one another. Measurement of the VV mass spectrum (here we generically denote $W^{\pm}, Z$ by V), would reveal a wealth of information about SEWS models, but is not feasible at the LHC or NLC.

This report focuses on the ability of a muon collider to distinguish between and perform detailed studies of SEWS models for longitudinal gauge-boson scattering. There may be additional large and easily observed signals in dynamical symmetry breaking models; for example, in Technicolor models both Technicolor hadrons [7] and techni-rho resonances [8,9] would be easily detected whenever the energy is adequate for them to be produced at a reasonable rate. Only the SEWS signals are addressed in the present report, based on the work of Ref. [10].

2 Overview of Models

Numerous models for the strongly interacting gauge sector have been considered. We focus on a selection of those considered in Ref. [2]:

- the Standard Model with a heavy Higgs boson of mass $m_H = 1$ TeV;
- a ("Scalar") model in which there is a spin-0, isospin-0 resonance with $M_S = 1$ TeV but non-SM width of $\Gamma_S = 350$ GeV;
- a ("Vector") model in which there is a spin-1, isospin-1 vector resonance with either $M_V = 1$ TeV and $\Gamma_V = 35$ GeV or $M_V = 2$ TeV and $\Gamma_V = 0.2$ TeV, but no spin-0 resonance. When necessary, we unitarize the model using K-matrix techniques as detailed in the Appendix.
- a model, denoted by LET-K or "$m_H = \infty$", in which the SM Higgs is taken to have infinite mass and the partial waves simply follow the behavior predicted by the low-energy theorems, except that the LET behavior is unitarized via the K-matrix techniques described in the Appendix.

We note that the $m_H = 1$ TeV Standard Model is the simplest VV scattering model for which the full kinematics and spin correlations among the final decay products are easily calculable. Consequently, this model is extremely useful in bench mark studies of the effectiveness of cuts and projection techniques. As discussed in Ref. [2], the distributions of the final V_L's, and their decay products, in other models should follow closely those found for the V_L's in the $m_H = 1$ TeV Standard Model. Thus, in analyzing the other SEWS models, we assume that cut efficiencies and distributions are the same as for the $m_H = 1$ TeV SM V_L's.

3 Rates and Motivations for Higher Energy

For a first estimate of the strong electroweak scattering effects we take the Standard Model with a heavy Higgs as a prototype of the strong scattering sector. For a 1 TeV SM

Higgs boson, the SEWS signal is accordingly defined as

$$\Delta\sigma = \sigma(m_H = 1 \text{ TeV}) - \sigma(\text{LH}) \ . \tag{1}$$

Results in the W^+W^- and ZZ channels for $\Delta\sigma$ (with no cuts of any kind) are shown in Table 1 for $\sqrt{s} = 1.5$ TeV (as often discussed for an e^+e^- collider) and 4 TeV. The strong scattering signal is relatively small at energies of order 1 TeV, but grows substantially as multi-TeV energies are reached. This is illustrated in Fig. 2, where $\sigma(m_H = 1 \text{ TeV})$ and $\sigma(\text{LH})$ are plotted separately. The signal $\Delta\sigma$ declines rapidly in magnitude for decreasing energy below $\sqrt{s} = 4$ TeV. The associated signal (S) and irreducible background event rates are given by $S = L\Delta\sigma$ and $L\sigma(\text{LH})$, where L is the integrated luminosity. Table 1 shows that a very respectable signal rate is achieved at 4 TeV and even before cuts the signal to irreducible background ratio is quite reasonable; both are much larger than at $\sqrt{s} = 1.5$ TeV. SEWS physics benefits from increasing energy in four ways.

- The luminosity for V_LV_L collisions is bremsstrahlung-initiated and grows at fixed subprocess $\hat{s} = M_{VV}^2$ as $1/\tau$ where $\tau = M_{VV}^2/s$.

- The SEWS amplitude function $A(\hat{s}, \hat{t}, \hat{u})$ typically increases as higher subprocess $\hat{s} = M_{VV}^2$ values become accessible; *e.g.* in the LET-K model $A(\hat{s}, \hat{t}, \hat{u}) \propto \hat{s}/v^2$, where v is the standard electroweak symmetry breaking parameter. This more than compensates for the slightly faster growth with s of the V_TV_T luminosity function (responsible for VV fusion backgrounds) $\propto \frac{1}{\tau}\ln^2\frac{s}{m_V^2}$ as compared to the V_LV_L luminosity.

- The background subprocess amplitudes typically have point-like $1/\hat{s}$ behavior and, further, some backgrounds are not proportional to the growing VV luminosities. In particular, many of the diagrams contributing to the amplitude for the irreducible light Higgs $V_TV_T + V_TV_L$ SM background do not have VV fusion topology.

- Finally, the luminosities at higher machine energies are normally designed to be larger to compensate for the $1/\hat{s}$ decline of the point-like subprocess cross sections for other types of new physics.

It appears that $\sqrt{s} = 4$ TeV is roughly the critical energy at which SEWS physics can first be studied in detail. This is especially true given that it will be desirable to impose strong cuts in order to maximize signal over background. Thus, the high energy reach of a muon collider could prove to be critically important.

Table 1. Strong electroweak scattering signals in $W^+W^- \to W^+W^-$ and $W^+W^- \to ZZ$ at future lepton colliders. Signal cross sections and the signal to irreducible LH background ratio are given for $L = 200$ fb^{-1} at $\sqrt{s} = 1.5$ TeV and $L = 1000$ fb^{-1} at $\sqrt{s} = 4$ TeV, with no cuts.

$\sqrt{s}$	$\Delta\sigma(W^+W^-)$	$[S/\text{LH}](W^+W^-)$	$\Delta\sigma(ZZ)$	$[S/\text{LH}](ZZ)$
1.5 TeV	8 fb	$\frac{1600}{8000}$	6 fb	$\frac{1200}{3600}$
4 TeV	80 fb	$\frac{80000}{170000}$	50 fb	$\frac{50000}{80000}$

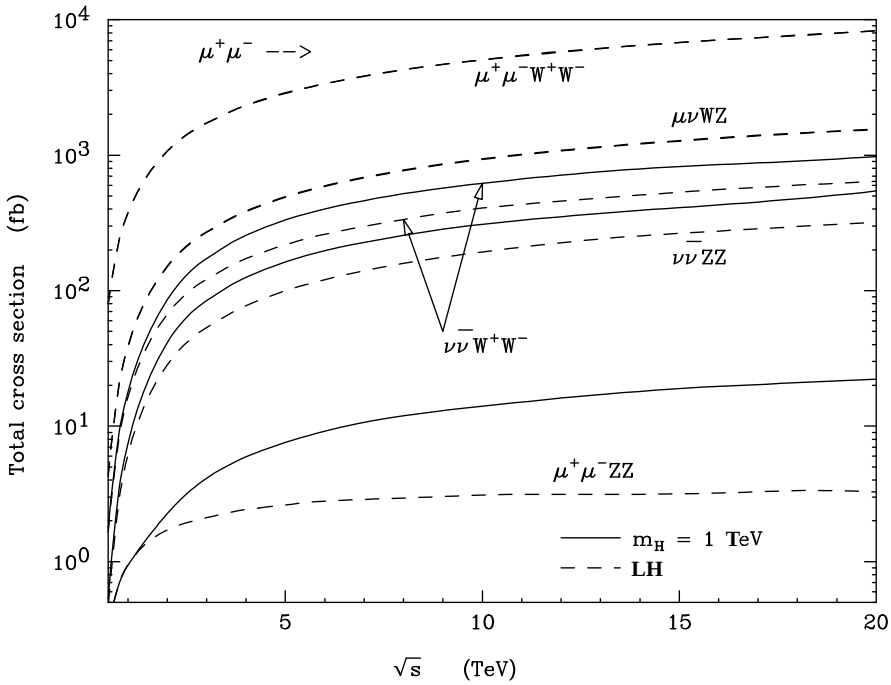

Figure 2. Signal and background cross sections as a function of $\sqrt{s}$ for strong $W^+W^- \to W^+W^-$ and $W^+W^- \to ZZ$ scattering as computed in the SM for $m_H = 1$ TeV at a $\mu^+\mu^-$ collider.

Table 2. Standard Model cross sections (in fb) at $\sqrt{s} = 4$ TeV in the W^+W^+ final state TT, TL and LL modes for a light Higgs compared to $m_H = 1$ TeV. Results are given both without any cuts and after imposing cuts I and II on the W^+'s as delineated in Section 4.

	LH				$m_H = 1$ TeV			
	TT	TL	LL	Sum	TT	TL	LL	Sum
No Cuts	48.9	26.9	6.75	82.6	49.5	26.5	12.1	88.1
With Cuts	1.34	0.19	0.03	1.56	1.36	0.15	1.51	3.02

The importance of high energy and signal selection cuts is particularly apparent in the W^+W^+ channel. We choose this channel to illustrate the polarization structure of the VV final state. In Table 2 we compare the polarization decomposition of the Standard Model W^+W^+ cross sections for the LH case with the $m_H = 1$ TeV SEWS model. (We define the vector boson polarizations in the VV rest frame.) With no cuts, substantial TL and not insignificant LL cross section components are present for the LH model, in addition to the dominant TT cross section. The increase ($\Delta\sigma$) in cross section in going to $m_H = 1$ TeV is a

small percentage of the total and is seen to be almost entirely in the LL final state (the TL contribution actually decreases). By imposing cuts on the W^+'s (specifically cuts I and II as delineated in Section 4), the TL and, especially, LL cross sections are reduced to negligible size compared to TT for the LH model. Further, with the cuts imposed, $\Delta\sigma$ is nearly as large as σ(LH). Thus, cuts are important both in reducing the background relative to the signal and also in isolating the LL component of the strongly interacting gauge boson cross section. Whether cuts are imposed or not, it is clear from Table 2 that the TT contribution to $\Delta\sigma$ is negligible. Finally, the magnitude of $\Delta\sigma$ in the W^+W^+ channel (even before cuts) becomes sufficient at $\sqrt{s} = 4$ TeV to allow quantitative study; for $\sqrt{s} \lesssim 1.5$ TeV $\Delta\sigma$ is so small that the W^+W^+ channel can at best provide only a hint of strong interactions among the gauge bosons.

4 Muon Collider Results using the Subtraction Procedure

For a $\mu^+\mu^-$ collider operating at 4 TeV the event rates and statistical significances for most channels markedly improve, the exception being the $W^\pm Z \to W^\pm Z$ channel. Table 3 summarizes our results for various SEWS models in the $W^+W^- \to W^+W^-$, $W^+W^- \to ZZ$ and $W^+W^+ \to W^+W^+$ channels[a] for the signal S and the full irreducible plus reducible background B event numbers obtained by summing over diboson invariant mass bins as specified in the caption. Also given is the statistical significance, $S/\sqrt{B}$, of the signals. The signal rate S is computed by subtracting the background rate B from the total event rate (signal+background) for a given SEWS model, see Eq. (1). The results presented in Table 3 are those obtained after imposing the following cuts, as detailed in Ref. [10].

The channel $W^\pm Z \to W^\pm Z$ is less interesting than the W^+W^-, W^+W^+ and ZZ channels for the following reasons. First, there is no direct s-channel scalar contribution to the $W^\pm Z$ process, unlike the processes W^+W^-, ZZ. Second, the LET-K $A(s,t,u)$ amplitude goes like t/v^2 which gives a smaller cross section than that of $W^+W^- \to ZZ$ or $W^+W^+ \to W^+W^+$ where $A(s,t,u) \propto s/v^2$. Even if there is an isospin-1 vector resonance, the W^+W^- final state will reveal a peak with the same strength as does the $W^\pm Z$ final state, with comparable backgrounds. Finally, the cuts we have discussed are not as successful for the $W^\pm Z \to W^\pm Z$ channel. In particular, the $p_T(VV)$ and $\mu^\pm$ veto cuts are no longer adequate to substantially suppress the (irreducible) background associated the $W^\pm\gamma \to W^\pm Z$ subprocess. Highly effective alternative cuts have not yet been identified.

In Figs. 3a–c we compare the M_{VV} distributions in the W^+W^-, ZZ and W^+W^+ final states for various SEWS models (including the combined reducible and irreducible backgrounds) to those for the combined background with all cuts, I–III, imposed. The SEWS models illustrated are the SM with $m_H = 1$ TeV, the unitarized $m_H = \infty$ (LET-K) model, and a Vector model with $M_V = 2$ TeV and $\Gamma_V = 0.2$ TeV. The numbers in Table 3 are obtained by integrating the distributions in these figures over the specified M_{VV} ranges, where the signal event numbers are those obtained after subtracting the background from the full SEWS model curves (which include the combined background). To indicate the accuracy with which the M_{VV} distributions could be measured, the $L = 200$ fb^{-1}, $\pm\sqrt{N}$ error bars associated with several 40 GeV bins for the LET-K model are shown.

[a] We focus on the $W^+W^+ \to W^+W^+$ like-sign channel, but the same results apply to the $W^-W^- \to W^-W^-$ channel. High luminosity $\mu^+\mu^+$ collisions may be somewhat easier to achieve.

Table 3. Total numbers of W^+W^-, ZZ and $W^+W^+ \to$ 4-jet signal (S) and background (B) events calculated for a 4 TeV $\mu^+\mu^-$ collider with integrated luminosity 200 fb^{-1} (1000 fb^{-1} in the parentheses), for cuts of $M_{VV} \geq 500$ GeV, $p_T(V) \geq 150$ GeV, $|\cos\theta_V| \leq 0.8$ and $p_T(WW) \geq 30$ GeV, $p_T(ZZ) \geq 20$ GeV. (For the case of a 2 TeV vector state, events for the W^+W^- channel are summed around the mass peak over the range $1.7 < M_{VV} < 2.3$ TeV.) Events containing a μ^+ or μ^- with $\theta_\mu \geq 12°$ and $E_\mu \geq 50$ GeV are vetoed. The signal rate S is that obtained by computing the total rate (including all backgrounds) for a given SEWS model and then subtracting the background rate; see Eq. (1). The statistical significance $S/\sqrt{B}$ is given for the signal from each model. The hadronic branching fractions of VV decays and the $W^\pm/Z$ identification/misidentification are included.

channels	Scalar $m_H = 1$ TeV $\Gamma_H = 0.5$ TeV	Vector $M_V = 2$ TeV $\Gamma_V = 0.2$ TeV	LET-K $m_H = \infty$ Unitarized
$\mu^+\mu^- \to \bar{\nu}\nu W^+W^-$			
S(signal)	2400 (12000)	180 (890)	370 (1800)
B(backgrounds)	1200 (6100)	25 (120)	1200 (6100)
$S/\sqrt{B}$	68 (152)	36 (81)	11 (24)
$\mu^+\mu^- \to \bar{\nu}\nu ZZ$			
S(signal)	1030 (5100)	360 (1800)	400 (2000)
B(backgrounds)	160 (800)	160 (800)	160 (800)
$S/\sqrt{B}$	81 (180)	28 (64)	32 (71)
$\mu^+\mu^+ \to \bar{\nu}\bar{\nu}W^+W^+$			
S(signal)	240 (1200)	530 (2500)	640 (3200)
B(backgrounds)	1300 (6400)	1300 (6400)	1300 (6400)
$S/\sqrt{B}$	7 (15)	15 (33)	18 (40)

From these plots and the sample error bars, it is apparent that, for any of the SEWS models investigated, the expected signal plus background could be readily distinguished from pure background alone on a bin by bin basis at better than 1σ all the way out to $M_{VV} = 2.5$ TeV (2 TeV) in the W^+W^- and W^+W^+ (ZZ) channels. Further, the small 2 TeV Vector model peak would be readily observed in the W^+W^- channel and its absence in the ZZ and W^+W^+ channels would be clear. Indeed, it would be feasible to determine the width of either a scalar or a vector resonance with moderate accuracy.

Currently discussed designs for the 4 TeV muon collider would provide luminosity of $L = 1000$ fb^{-1} per year. Even if this goal is not reached, one might reasonably anticipate accumulating this much luminosity over a period of several years. For $L = 1000$ fb^{-1}, the accuracy with which the M_{VV} distributions can be measured becomes very remarkable. To illustrate, we plot in Figs. 4a-b, the signal plus background in the $m_H = 1$ TeV, $\Gamma_H = 0.5$ TeV SM and the $M_S = 1$ TeV, $\Gamma_S = 0.35$ TeV Scalar resonance model, and the combined background, taking $L = 1000$ fb^{-1} and using an 80 GeV bin size (so as to increase statistics on a bin by bin basis compared to the 40 GeV bin size used in the previous figures). The error bars are almost invisible for $M_{VV} \lesssim 1.5$ TeV, and statistics is more than adequate to distinguish between the $\Gamma_H = 500$ GeV SM resonance and a $\Gamma_S = 350$ GeV Scalar model at a resonance mass of 1 TeV. Indeed, we estimate that the width could be measured to better

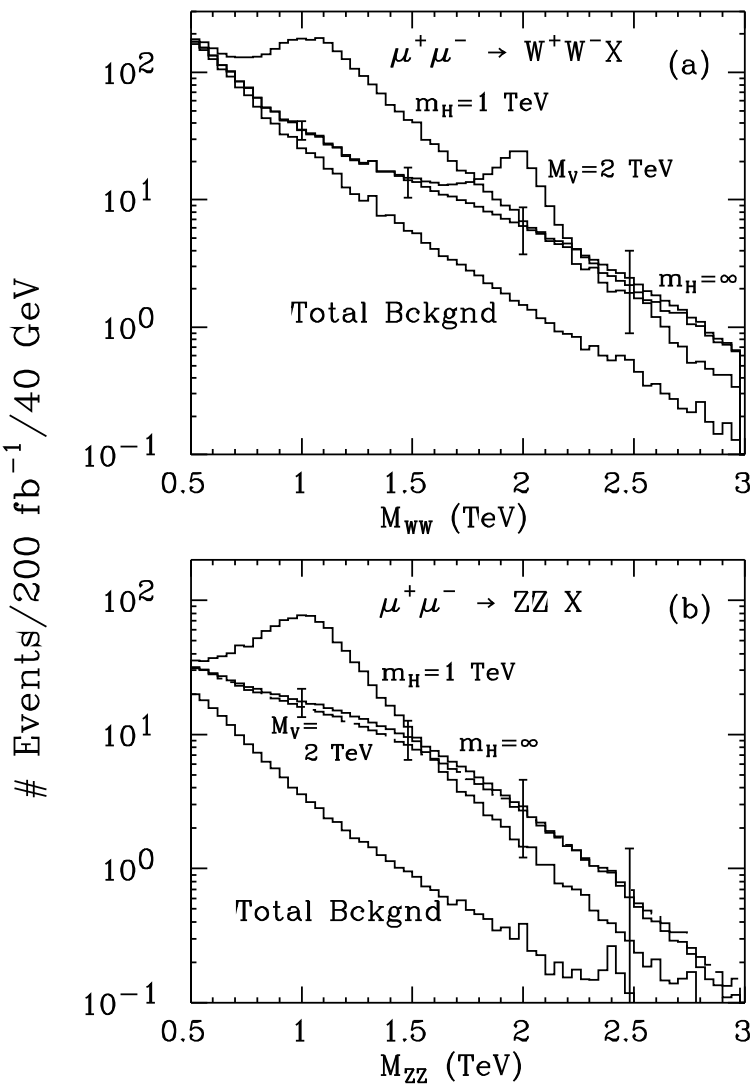

Figure 3. Number of events at $\sqrt{s} = 4$ TeV and $L = 200$ fb^{-1} versus M_{VV} for SEWS models (including the combined backgrounds) and for the combined backgrounds alone in the (a) W^+W^- and (b) ZZ final states after imposing all cuts, I–III. Sample signals shown are: (i) the SM Higgs with $m_H = 1$ TeV; (ii) the SM with $m_H = \infty$ unitarized via K-matrix techniques (LET-K model); and (iii) the Vector model with $M_V = 2$ TeV and $\Gamma_V = 0.2$ TeV. In the ZZ final state the histogram for (iii) falls just slightly lower than that for model (ii) at lower M_{VV}. Sample statistical uncertainties for the illustrated 40 GeV bins are shown in the case of the $m_H = \infty$ model.

than ± 30 GeV. Further, for such small errors we estimate that a vector resonance could be seen out to nearly $M_V \sim 3$ TeV. This ability to measure the M_{VV} distributions with high precision would allow detailed insight into the dynamics of the strongly interacting

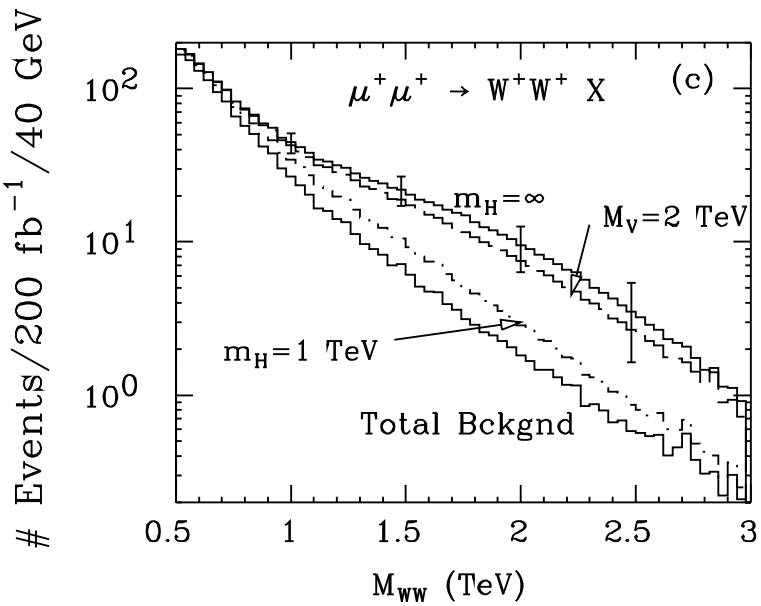

Figure 3. (continued) Events as a function of M_{VV} for sample SEWS models (including the combined backgrounds) and for the combined backgrounds alone in the (c) W^+W^+ final state after imposing all cuts, I–III. See caption for Fig. 3a-b.

electroweak sector. Thus, if some signals for a strongly interacting sector emerge at the LHC, a $\sqrt{s} = 3-4$ TeV $\mu^+\mu^-$ collider will be essential.

It is important to measure the M_{VV} spectrum in all three (W^+W^-, ZZ and W^+W^+) channels in order to fully reveal the isospin composition of the model. For instance, the Vector model and the LET-K model yield very similar signals in the ZZ and W^+W^+ channels, and would be difficult to separate without the W^+W^- channel resonance peak. More generally, the ratio of resonance peaks in the ZZ and W^+W^- channels would be needed to ascertain the exact mixture of Vector (weak isospin 1) and Scalar (isospin 0) resonances should they be degenerate. Determination of the isospin composition of a non-resonant model, such as the LET-K model, requires data from all three channels. The ZZ channel can only be separated from the W^+W^- channel if the jet energy resolution is reasonably good.

5 Summary and Conclusion

Achieving VV scattering subprocess energies above $1-2$ TeV is critical for studies of strongly interacting electroweak sector (SEWS) models, and is only possible with high event rates at lepton-antilepton (e^+e^- or $\mu^+\mu^-$ colliders) or quark-antiquark (hadron collider) subprocess energies of order $3-4$ TeV. Consequently, a muon collider facility with center of mass energy $\sqrt{s} \sim 3-4$ TeV and luminosity $L = 200-1000$ fb^{-1} allowing both $\mu^+\mu^-$ and $\mu^+\mu^+$ (or $\mu^-\mu^-$) collisions would be a remarkably powerful machine for probing a strongly interacting electroweak sector (SEWS). The LHC or a lower energy e^+e^- collider would not be competitive.

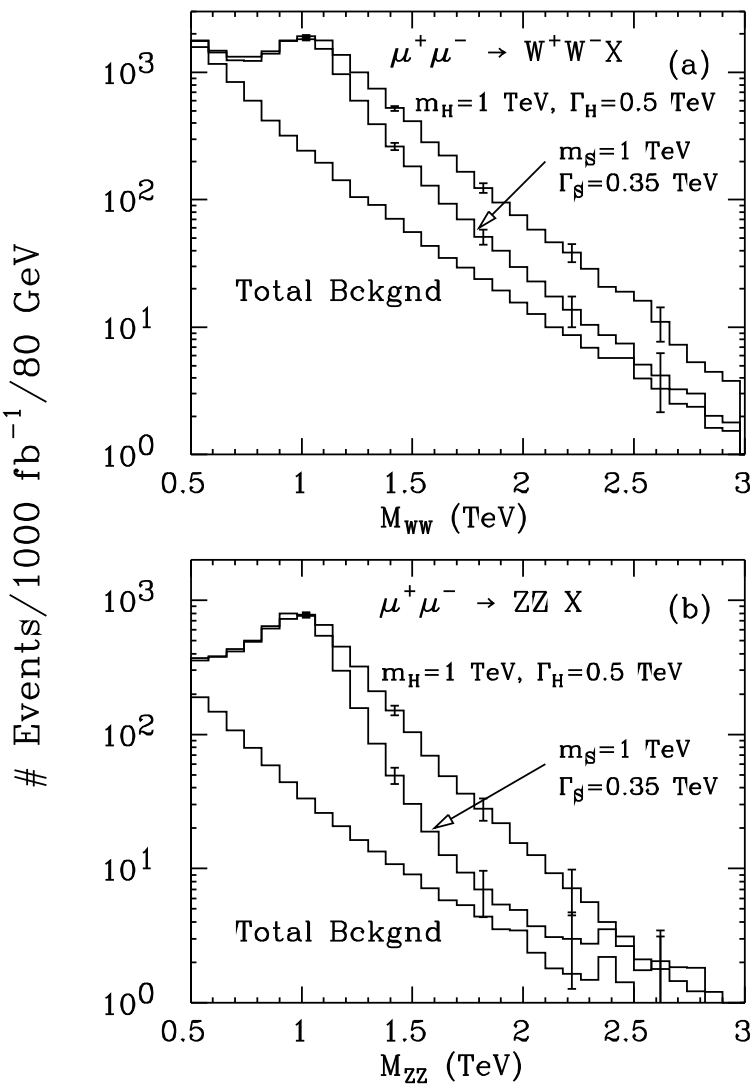

Figure 4. Events versus M_{VV} for two SEWS models (including the combined backgrounds) and for the combined backgrounds alone in the (a) W^+W^- and (b) ZZ final states after imposing all cuts, I–III. Signals shown are: (i) the SM Higgs with $m_H = 1$ TeV, $\Gamma_H = 0.5$ TeV; (ii) the Scalar model with $M_S = 1$ TeV, $\Gamma_S = 0.35$ TeV. Results are for $L = 1000$ fb^{-1} and $\sqrt{s} = 4$ TeV. Sample error bars are shown at $M_{VV} = 1.02$, 1.42, 1.82, 2.22 and 2.62 TeV for the illustrated 80 GeV bins.

Event rates for even the weakest of the model signals studied are such that the M_{VV} distributions could be quantitatively delineated, thereby providing a direct measurement of the underlying strong VV interaction amplitude as a function of the VV subprocess energy and strong differentiation among various possible models of the strongly interacting

electroweak sector.

Thus, if evidence for a strongly interacting electroweak sector emerges from LHC data, construction of a high luminosity, high energy muon collider should be given the highest priority.

ACKNOWLEDGMENTS

We thank M. Berger and J. Gunion for collaborations that had led to the original work reported here. This work was supported in part by the U.S. Department of Energy under Grants No. DE-FG02-95ER40896 and in part by the Wisconsin Alumni Research Foundation.

REFERENCES

References

1. D. A. Dicus and V. S. Mathur, Phys. Rev. **D7**, 3111 (1973); B. W. Lee, C. Quigg, and H. Thacker, Phys. Rev. **D16**, 1519 (1977); M. Veltman, Acta Phys. Polon. **B8**, 475 (1977); M. S. Chanowitz and M. K. Gaillard, Nucl. Phys. **B261**, 379 (1985).
2. J. Bagger, V. Barger, K. Cheung, J.F. Gunion, T. Han, G.A. Ladinsky, R. Rosenfeld, and C.-P. Yuan, Phys. Rev. **D49**, 1246 (1994); *ibid.* **D52**, 3878 (1995).
3. V. Barger *et al.*, Phys. Rev. **D42**, 3052 (1990); V. Barger *et al.*, Phys. Rev. **D44**, 1426 (1991); *ibid.* Phys. Rev. **D44**, 2701 (1991); D. Dicus, J. Gunion, and R. Vega, Phys. Lett. **B258**, 475 (1991); M. Berger and M. Chanowitz, Phys. Lett. **B263**, 509 (1991); D. Dicus *et al.*, Nucl. Phys. **B377**, 31 (1992); M. S. Chanowitz and W. Kilgore, Phys. Lett. **B322**, 147 (1994); *ibid.* **B347**, 387 (1995).
4. ATLAS Collaboration, Technical Proposal, CERN/LHCC/94-13; ATLAS Internal Note PHYS-NO-033; CMS Collaboration, Technical Proposal, CERN/LHCC/94-38.
5. V. Barger, K. Cheung, T. Han, and R.J.N. Phillips, Phys. Rev. **D52**, 3815 (1995).
6. J. Gunion and A. Tofighi-Niaki, Phys. Rev. **D36**, 2671 (1987); *ibid.* **D38**, 1433 (1988); K. Hagiwara, J. Kanzaki and H. Murayama, KEK-TH-282 (1991); V. Barger, K. Cheung, B.A. Kniehl and R.J.N. Phillips, Phys. Rev. **D46**, 3725 (1992); Y. Kurihara and R. Najima, Phys. Lett. **B301**, 292 (1993).
7. E. Eichten, I. Hinchliffe, K. Lane and C. Quigg, Phys. Rev. **D34**, 1547 (1986); K. Lane, BUHEP-94-2, 1993 TASI Lectures (World Scientific), and references therein.
8. A. Dobado, M. J. Herrero, J. Terron, Z. Phys. **C50**, 465 (1991); R. Casalbuoni *et al.*, Phys. Lett. **B249**, 130 (1990); hep-ph/9502325 (Aug. 1994).
9. T. Barklow, in the Albuquerque DPF94 Meeting, ed. by Sally Seidel, p. 1236, and references therein.
10. V. Barger, M.S. Berger, J.F. Gunion and T. Han, Phys. Rev. **D55**, 142 (1997).
11. J.F. Gunion, B. Grzadkowski, X.-G. He, UCD-96-14.
12. Particle Data Group, L. Montanet et al., Phys. Rev. **D50**, 1173 (1994).
13. For a review of unitarization schemes, see *e.g.* K.-I. Hikasa, in *Physics and Experiments with Linear Colliders*, Saariselka, Finland, September 1992, ed. R. Orava *et al.*, World Scientific, p. 451.